Improved Monitoring of Industrial Processes With Robust Control Statistics

Fernanda Figueiredo

CEAUL and Faculdade de Economia da Universidade do Porto

and

M. Ivette Gomes

CEAUL and DEIO (FCUL), Universidade de Lisboa

Abstract. The Shewhart control charts are the most popular tools in Statistical Process Control (SPC) used for monitoring industrial processes. They are usually developed under the assumptions of independent and normally distributed data, which rarely hold true in practice, and are usually implemented with estimated control limits. As in general we mainly want to control the process mean value and the process standard deviation independently of the data distribution, it seems sensible to advance with control charts based on robust statistics to monitor the process parameters, more resistant to moderate changes in the underlying process distribution. In this study we investigate the advantage of using control charts based on robust statistics together with the use of robust estimates for the target process values under control. Apart from the traditional control charts, the sample mean chart and the sample range chart, we consider robust control charts based on the total median and on the total range statistics for monitoring the process mean value and the process standard deviation. Through the use of Monte Carlo simulations we compare all these charts in terms of robustness and performance. Finally we illustrate the behavior of these charts when implemented to monitor a cork process production.

AMS 2000 subject classification: 62G05, 62G35, 62P30, 65C05.

Keywords: Statistical Process Control; Control Charts; Robust Estimation.

1 Introduction

For monitoring industrial processes, or more precisely, a quality characteristic X, at the targets μ_0 and σ_0, the mean value and the standard deviation of the process X, respectively, the most commonly used charts are the Shewhart control charts with 3-sigma control limits. These charts are usually developed under the assumptions of independent and normally distributed data, and have control limits of the form

$$CL's = E(W) \pm 3\sqrt{V(W)}, \tag{1.1}$$

where W, E and V denote the control statistic of the chart, its expected value and its variance, respectively. More precisely, to monitor the process mean value (μ) it is common to implement a two-sided sample mean chart, $\overline{X}$, also denoted M-chart, with lower and upper control limits given by

$$LCL_M = \mu_0 - 3\sigma_0/\sqrt{n}, \quad UCL_M = \mu_0 + 3\sigma_0/\sqrt{n}. \tag{1.2}$$

To monitor the process standard deviation (σ) it is common to implement a sample range chart, $\overline{R}$, with lower and upper control limits given by

$$LCL_R = d_2\sigma_0 - 3d_3\sigma_0, \quad UCL_R = d_2\sigma_0 + 3d_3\sigma_0, \tag{1.3}$$

where d_2 and d_3 are the constants tabulated for standard normal data presented in Table 2 for the most common sample sizes n. General details about control charts may be found, for instance, in Montgomery (2005) and in Ryan (2000).

For normal data and when it is not necessary to estimate the control limits, the Shewhart control charts present a reasonable high performance in detecting moderate to large changes that can occur in the process parameters. However, despite of the importance of the normal distribution in SPC, the experience tells us that even in potential normal situations there is some possibility of having an underlying non-normal distribution, with moderate to strong asymmetry and with tails heavier than the normal tail, as well as a significant correlation between the observations.

Additionally, in practice the target values μ_0 and σ_0 are not fixed given values, and we have to estimate them to determine the control limits of the chart. Several studies refer that to obtain control charts with estimated control limits with the same properties as the correspondent charts with true limits, even for normal

data, we must use a large number of initial subgroups in the estimation, and we must determine the control limits in a robust way in order to minimize the effect of possible outliers in the initial subgroups. The effect of the estimation of the control limits and of the non-normality in the performance of the usual control charts can be found in Rocke (1989, 1992), Quesenberry (1993), Amin and Lee (1999), Nedumaran and Pignatiello (2001), Chakraborti (2000, 2006), Champ and Jones (2004), Figueiredo and Gomes (2004, 2006) and Jensen *et al.* (2006), among others. Schilling and Nelson (1976), Balakrishnan and Kocherlakota (1986) and Chan et *al.* (1988) provide some corrections to the control limits of the usual control charts in order to maintain the expected false alarm rate when monitoring non-normal data.

To sum up the traditional control charts must be used carefully, being important to verify as far as the assumptions associated to the implementation of the traditional charts are fulfilled by the data process, in order to decide for the implementation of a control chart for the specific distribution whenever it seems necessary, or instead, for the implementation of a robust control chart, less-sensitive to the normality assumption and to the estimation of unknown parameters.

In this study we shall investigate the benefits of using control charts based on robust control statistics, so that we do not have either a very high or a very low false alarm rate whenever the parameters to be controlled are close to the targets, although the data is no longer normal, together with the use of robust estimates for the target values under control. Some considerations about "robust" estimation can be found in Hampel (1971), Lax (1985), Hoaglin *et al.* (1983), Hampel *et al.* (1986), Figueiredo (2003a, 2003b) and Figueiredo and Gomes (2004), among others. The design of some "robust" control charts can be found in Rocke (1989, 1992) and in Figueiredo and Gomes (2004, 2006), for instance.

In Section 2 we provide some information about the total median and the total range statistics, considered in this study to estimate and to monitor the process mean value and the process standard deviation, together with the sample mean and the sample range statistics. We analyze the robustness and efficiency of these location and scale estimators, as well as their sampling distribution. In Section 3 we present some simulation results about the robustness and the performance of some control charts, and in Section 4 we compare their performance to monitor a cork process production.

2 The total median and the total range statistics

Let us denote $(X_1, \cdots, X_n)$ a random sample of size n taken from a process X with distribution function (d.f.) F, and $(X_{(1)}, \cdots, X_{(n)})$ the random sample of the associated ascending order statistics (o.s.). Given an observed sample $(x_1, \cdots, x_n)$, the random associated bootstrap sample, $(X_1^*, \cdots, X_n^*)$, is a random sample of independent, identically distributed (i.i.d.) replicates from a random variable (r.v.) X^*, with distribution function equal to the empirical d.f. of our observed sample, i.e., given by

$$F_n^*(x) = \frac{1}{n} \sum_{i=1}^{n} I_{\{x_i \leq x\}}, \quad \text{with } I_A = \begin{cases} 1 & \text{if } A \text{ occurs} \\ 0 & \text{otherwise} \end{cases}$$

the indicator function of the set A.

Definition 2.1. *The bootstrap median, i.e., the median of the bootstrap sample, is given by*

$$BMd = \begin{cases} X_{(m)}^* & \text{if } n = 2m-1, \\ \left(X_{(m)}^* + X_{(m+1)}^*\right)/2 & \text{if } n = 2m, \end{cases} \qquad m = 1, 2, \cdots$$

and the bootstrap range, i.e., the range of the bootstrap sample, is given by

$$BR = X_{(n)}^* - X_{(1)}^*.$$

Remark 2.1. *Note that given an observed sample $(x_1, \cdots, x_n)$, the support of the bootstrap median is the set $\left\{(x_{(i)} + x_{(j)})/2,\, 1 \leq i \leq j \leq n\right\}$, and the support of the bootstrap range is the set $\left\{x_{(j)} - x_{(i)},\, 1 \leq i \leq j \leq n\right\}$.*

Let us denote α_{ij} and β_{ij} the following probabilities:

$$\alpha_{ij} = P\left(BMd = \frac{x_{(i)} + x_{(j)}}{2}\right), \, 1 \leq i \leq j \leq n, \tag{2.1}$$

$$\beta_{ij} = P\left(BR = x_{(j)} - x_{(i)}\right), \, 1 \leq i < j \leq n, \tag{2.2}$$

with $P(A)$ denoting the probability of the event A. Cox and Iguzquiza (2001) and Figueiredo and Gomes (2004, 2006) present explicit expressions for α_{ij} and β_{ij}.

Definition 2.2. *The total median statistic, here denoted TMd, is given by*

$$TMd := \sum_{i=1}^{n} \sum_{j=i}^{n} \alpha_{ij} \, \frac{X_{(i)} + X_{(j)}}{2} = \sum_{i=1}^{n} a_i X_{(i)}, \tag{2.3}$$

and the total range statistic, here denoted TR, is given by

$$TR := \sum_{i=1}^{n-1} \sum_{j=i+1}^{n} \beta_{ij}(X_{(j)} - X_{(i)}) = \sum_{i=1}^{n} b_i X_{(i)}, \tag{2.4}$$

where the coefficients a_i and b_i are given by $a_i = \frac{1}{2}\left(\sum_{j=i}^{n} \alpha_{ij} + \sum_{j=1}^{i} \alpha_{ji}\right)$ and $b_i = \sum_{j=1}^{i-1} \beta_{ji} - \sum_{j=i+1}^{n} \beta_{ij}$, $1 \leq i \leq n$.

Remark 2.2. *Note that the coefficients a_i and b_i are independent of the underlying model F, depending only on the sample size n. A linear combination of the sample o.s. with weights given by these coefficients, such as the TMd or the TR statistics, define a kind of "robust" trimmed-mean or "robust" range, where the percentage of trimming is determined independently of the underlying distribution of the data. The extreme observations have a smaller influence in these statistics than in the sample mean or in the sample range statistics, and thus they can be used to estimate the location and the scale parameters when there is a possibility of having some disturbances in the data such as some outliers or contaminated data. In Table 1 we present, for each entry i, the values of the coefficients a_i and b_i with three decimal figures, for the most usual sample sizes n in SPC.*

Table 1: Coefficients a_i and b_i, $a_i = a_{n-i+1}$ and $b_i = -b_{n-i+1}$.

$i \diagup n$		3	4	5	6	7	8	9	10
1	a_i	0.259	0.156	0.058	0.035	0.010	0.007	0.001	0.001
	b_i	-0.750	-0.690	-0.672	-0.666	-0.661	-0.657	-0.653	-0.652
2	a_i	0.482	0.344	0.259	0.174	0.098	0.064	0.029	0.019
	b_i	0.000	-0.198	-0.240	-0.246	-0.245	-0.244	-0.242	-0.241
3	a_i			0.366	0.291	0.239	0.172	0.115	0.078
	b_i			0.000	-0.058	-0.073	-0.077	-0.078	-0.079
4	a_i					0.306	0.257	0.221	0.168
	b_i					0.000	-0.016	-0.020	-0.022
5	a_i							0.268	0.234
	b_i							0.000	-0.004

2.1 Location and scale estimators: robustness and efficiency

Several Monte Carlo simulation studies have been carried out to evaluate the efficiency and the robustness of some location and scale estimators, including the total median and the total range statistics. Some of these studies are presented in Figueiredo (2003a, 2003b) and in Figueiredo and Gomes (2004, 2006), for a reasonably large set of symmetric and asymmetric distributions, with different skewness and tail weight.

Remark 2.3. *To compare the efficiency of the different location estimators we have evaluated their mean square error; since this measure is affected by the scaling of the estimator, to compare the scale estimators we have computed the variance of the logarithm of the estimator. Details about performance measures of scale estimators can be found in Lax (1985).*

Remark 2.4. *To select the most robust estimator among the estimators under study we applied the following Max/Min criterion: first, for every distribution we obtain the most efficient estimator, among the ones considered; then, we compute the efficiency of the other estimators relatively to the best one, previously selected; next, for each estimator we save the obtained minimum relative efficiency along all the considered set of distributions, i.e., the "degree of robustness"of the estimator; finally, the most robust estimator is the one with the highest "degree of robustness".*

From the results of these studies we conclude that the TMd statistic can be used to estimate the median value of a distribution F, as well as the mean value of a symmetric or approximately symmetric distribution; the TR statistic can be used to estimate the process standard deviation. Note that the R and the TR statistics are biased estimators for the standard deviation; for providing an unbiased estimate whenever the underlying model F is normal, we consider standardized versions of these statistics, obtained by the division of R and TR by a scale constant. These constants are equal to the statistic expected value for the standard normal distribution (here denoted by $d_2 \equiv d_{2,R}$ and $d_{2,TR}$, respectively), and are given in Table 2, together with the statistic standard deviation (here denoted by $d_3 \equiv d_{3,R}$, $d_{3,TR}$ and $d_{3,TMd}$), for the most common values of n.

Table 2: Expected value, $d_{2,\bullet}$, and standard deviation, $d_{3,\bullet}$, of the R, TR and TMd statistics for standard normal distribution; $d_{2,TMd} = 0$.

Constants	3	4	5	6	7	8	9	10
d_2	1.693	2.059	2.326	2.534	2.704	2.847	2.970	3.078
$d_{2,TR}$	1.269	1.538	1.801	2.027	2.210	2.364	2.491	2.610
d_3	0.888	0.880	0.864	0.848	0.833	0.820	0.808	0.797
$d_{3,TR}$	0.666	0.653	0.657	0.659	0.656	0.650	0.641	0.636
$d_{3,TMd}$	0.583	0.507	0.464	0.425	0.401	0.375	0.359	0.340

To analyze the robustness of the previous statistics, and following the methodology presented in Figueiredo (2003b) and Figueiredo and Gomes (2004), we consider several symmetric distributions, related with the standard normal distribution, and with different tail-weights τ, an indicator defined in (2.5), . More precisely, we consider standardized data of the following set D of symmetric distributions:

1. the standard normal, N(0,1);
2. the standard logistic, Log(0,1);
3. the Student-t distributions, t_ν, with 3, 5 and 10 degrees of freedom, ν;
4. the contaminated normal distributions, $CN(\alpha 100\%)$, in which each observation has a $(1-\alpha)100\%$ probability of being drawn from the N(0,1) and $\alpha 100\%$ probability of being drawn from the N(0,k), with percentages of contamination, α, of 0.01, 0.05 and 0.10, and a standard deviation k of 3.

Note that even in potential normal situations there is some possibility of having disturbances in the data, and one of the previous distributions in D, for instance, could describe the process data in a more reliable way.

Definition 2.3. *The tail-weight coefficient of a distribution F, here denoted τ, is given by*

$$\tau := \frac{1}{2} \frac{\frac{F^{\leftarrow}(0.99)-F^{\leftarrow}(0.5)}{F^{\leftarrow}(0.75)-F^{\leftarrow}(0.5)} + \frac{F^{\leftarrow}(0.5)-F^{\leftarrow}(0.01)}{F^{\leftarrow}(0.5)-F^{\leftarrow}(0.25)}}{\frac{\Phi^{\leftarrow}(0.99)-\Phi^{\leftarrow}(0.5)}{\Phi^{\leftarrow}(0.75)-\Phi^{\leftarrow}(0.5))}}, \tag{2.5}$$

where $F^{\leftarrow}$ *and* $\Phi^{\leftarrow}$ *denote the inverse functions of* F *and of the standard normal distribution function* Φ*, respectively. For symmetric distributions we have* $\tau = \frac{F^{\leftarrow}(0.99)}{F^{\leftarrow}(0.75)} / \frac{\Phi^{\leftarrow}(0.99)}{\Phi^{\leftarrow}(0.75)}$*, the tail-weight coefficient defined in Hoaglin et al. (1983).*

In Figure 1 we present the most efficient estimator for the mean value and for the standard deviation of a distribution F in D, for sample sizes 3 up to 10; in Figure 2 we picture the degree of robustness of the previous estimators. Apart from the $M \equiv \overline{X}$ and the TMd location estimators we have considered the sample median estimator, Md, and apart from the R and the TR scale estimators we have considered the sample standard deviation estimator, S.

		sample size							
τ_F	F	3	4	5	6	7	8	9	10
1,72	$t_{(3)}$	Md	Md	TMd	TMd	TMd	TMd	TMd	TMd
1,54	CN(10%)	TMd	TMd	TMd	TMd	TMd	TMd	TMd	TMd
1,34	t(5)	TMd	TMd	TMd	TMd	TMd	TMd	TMd	TMd
1,21	Log(0,1)	TMd	TMd	TMd	TMd	TMd	TMd	TMd	TMd
1,20	CN(5%)	TMd	TMd	TMd	TMd	TMd	TMd	TMd	M
1,15	$t_{(10)}$	TMd	TMd	TMd	TMd	M	M	M	M
1,03	CN(1%)	TMd	TMd	M	M	M	M	M	M
1,00	N(0,1)	M	M	M	M	M	M	M	M

		sample size							
τ_F	F	3	4	5	6	7	8	9	10
1,72	$t_{(3)}$	TR	TR	TR	TR	TR	TR	TR	TR
1,54	CN(10%)	TR	TR	TR	TR	TR	TR	S	S
1,34	t(5)	TR	TR	TR	TR	TR	TR	S	S
1,21	Log(0,1)	TR	TR	TR	TR	TR	S	S	S
1,20	CN(5%)	TR	TR	TR	TR	TR	S	S	S
1,15	$t_{(10)}$	TR	TR	TR	S	S	S	S	S
1,03	CN(1%)	TR	S	S	S	S	S	S	S
1,00	N(0,1)	S	S	S	S	S	S	S	S

Figure 1: Most efficient estimator for the mean value (left) and for the standard deviation (right).

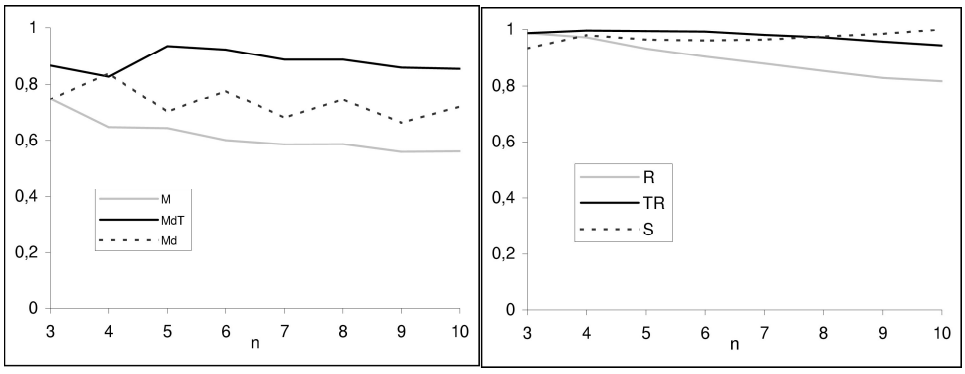

Figure 2: Degree of robustness of the location (left) and scale (right) estimators under study.

From these figures we can observe that the TMd-estimator is much more robust to changes in the underlying distribution F than the sample mean and the sample median estimators, M and Md. The TR-estimator and the S-estimator present similar degree of robustness when we consider any distribution F in D as possible to describe the data process, and are more robust than the R-estimator. The TMd and the TR estimators are the most efficient to estimate the mean value and the standard deviation of a moderate-to-heavy tailed distribution, respectively; we advise the use of the M and of the S estimators only for distributions with small tail-weight and moderate-to-large sample sizes; in the extreme case of small samples and too heavy tailed distributions, the sample median and the total range turn out to be the most efficient location and scale estimator, respectively. The R-estimator is not at all competitive, although in SPC the range control chart based on the R-statistic is much more popular to monitor the standard deviation than the standard deviation control chart, based on the S-statistic.

2.2 The sampling distribution

In order to get information about the sampling distribution of the previous location and scale statistics $M \equiv \overline{X}$, TMd, R and TR, here generically denoted by W, we generated 50,000 values of each of the statistics W, for sample sizes $n = 5, 10$, and some distributions of X belonging to the set D. We simulated their density sampling distribution, and we estimated the tail-weight, τ, defined in (2.5), and the asymmetry through the use of the Pearson and of the Bowley skewness coefficients, γ and γ_B, defined in (2.6) and (2.7), respectively.

Definition 2.4. *The Fisher skewness coefficient of a distribution F, here denoted γ, is given by*

$$\gamma := \frac{\mu_3}{\mu_2^{3/2}}, \tag{2.6}$$

where μ_r denotes the r-th central moment of F; the Bowley skewness coefficient (also denoted quartile skewness coefficient), here denoted γ_B, is given by

$$\gamma_B := \frac{(F^{\leftarrow}(0.75) - F^{\leftarrow}(0.5)) - (F^{\leftarrow}(0.5) - F^{\leftarrow}(0.25))}{F^{\leftarrow}(0.75) - F^{\leftarrow}(0.25)}. \tag{2.7}$$

The obtained estimates of the parameters τ, γ and γ_B, and of the quantiles $\chi_p \equiv F^{\leftarrow}(p)$, $p = 0.1\%, 1\%, 25\%, 50\%, 75\%, 99\%$ and 99.9%, of the sampling distribution of the statistics under study, are presented in Tables 3-6. In Figures 3-6 we present some of histograms associated to these simulated sampling distributions.

Table 3: Estimates of τ, γ, γ_B, $\chi_{0.1\%}$, $\chi_{1\%}$, $\chi_{25\%}$, $\chi_{50\%}$, $\chi_{75\%}$, $\chi_{99\%}$, $\chi_{99.9\%}$, for the M sampling distribution and sample sizes $n = 5, 10$.

F	n	τ	γ	γ_B	$\chi_{0.1\%}$	$\chi_{1\%}$	$\chi_{25\%}$	$\chi_{50\%}$	$\chi_{75\%}$	$\chi_{99\%}$	$\chi_{99.9\%}$
N(0,1)	5	1.00	0.01	0.00	-1.398	-1.039	-0.302	-0.001	0.297	1.046	1.410
	10	0.99	-0.01	0.00	-0.977	-0.733	-0.217	-0.001	0.212	0.734	0.962
Log(0,1)	5	1.06	-0.02	-0.02	-2.677	-1.966	-0.538	0.004	0.531	1.927	2.696
	10	1.03	0.01	0.01	-1.827	-1.350	-0.378	0.001	0.387	1.365	1.824
t_3	5	1.33	-1.07	0.00	-2.120	-1.122	-0.247	-0.003	0.243	1.133	2.397
	10	1.21	-0.34	0.00	-1.408	-0.773	-0.185	-0.000	0.185	0.777	1.410
t_5	5	1.11	0.04	0.00	-1.577	-1.097	-0.287	-0.002	0.284	1.093	1.561
	10	1.06	0.03	0.00	-1.091	-0.753	-0.205	0.000	0.207	0.760	1.086
t_{10}	5	1.05	-0.02	0.00	-1.456	-1.071	-0.288	0.007	0.300	1.061	1.485
	10	1.02	0.01	0.00	-1.004	-0.734	-0.210	0.000	0.209	0.743	1.042
CN(1%)	5	1.03	0.02	-0.01	-1.582	-1.090	-0.312	0.000	0.305	1.099	1.576
	10	1.00	-0.02	0.00	-0.968	-0.746	-0.212	0.002	0.216	0.731	0.975
CN(5%)	5	1.14	-0.02	0.01	-2.025	-1.316	-0.331	0.001	0.336	1.309	1.942
	10	0.99	-0.01	0.01	-0.999	-0.737	-0.213	0.000	0.215	0.731	0.975
CN(10%)	5	1.21	0.00	-0.01	-2.370	-1.523	-0.373	-0.007	0.355	1.526	2.235
	10	0.99	0.00	0.00	-0.957	-0.736	-0.214	0.000	0.214	0.733	0.964

From the values in Table 3 we observe that the sampling distribution of the M-statistic is approximately symmetric for the models under study, except for the t_3 distribution; in this case we obtained a negative skewed sampling distribution, but its central part is symmetric as we conclude from the obtained quartile skewness coefficient, $\gamma_B \simeq 0$, and from the histogram of the simulated density function.

When we consider underlying models F with small tail-weight, such as the normal, the logistic, the t_{10} and the $CN(1\%)$ model, the sampling distribution of M presents the same tail-weight as the normal distribution; for distributions F with moderate-to-heavy tails, such as the t_3, the t_5, the $CN(5\%)$ and the $CN(10\%)$, the sampling distribution of M has tails heavier than the normal tail, but not so heavy as the tails of the underlying distribution, and this tail-weight decreases as the sample size n increases. For non-normal models the obtained lower quantiles of the sampling distribution of M, $\chi_{0.1\%}$ and $\chi_{1\%}$, are smaller than the corresponding quantiles obtained in the normal case, and the upper quantiles, $\chi_{99\%}$ and $\chi_{99.9\%}$, are larger than the corresponding normal quantiles. This reveals the weak robustness of the M statistic to changes in the underlying model, principally for small values of n. Finally, the interval of variation of the sampling distribution of the M statistic for non-normal data is larger than in the normal case, but the interquartile range is almost the same for all the distributions; thus, the significant differences between the several sampling distributions are in the tails, and this fact is very important when we are interested in the estimation of high quantiles, as usually happens in Statistical Quality Control, for instance.

From Table 4 we note that the sampling distribution of the TMd-statistic is symmetric for all the models under study, even when we consider heavy-tailed underlying models F, such as the t_3 and the $CN(10\%)$, for instance. Thus, the chance of having an extreme value from the TMd sampling distribution is smaller than the chance of obtaining it from the M sampling distribution. For large sample sizes of contaminated normal data, say $n = 10$, the lower and the upper quantiles of the TMd distribution are similar to the corresponding normal quantiles, but for $n = 5$ there are significant differences; thus we do not advise the use of the TMd statistic in SPC for very small values of n, when there is some possibility of having contaminated normal data. For the logistic model the interval of variation of the sampling distribution of the TMd statistic is larger than in the normal case, as well as the interquartile range, and we have the opposite situation for Student-t models; even so, the differences to the normal case are smaller when we consider the TMd instead of the M statistic. Some of these conclusions can be observed from the histograms presented in Figures 3-6.

Table 4: Estimates of τ, γ, γ_B, $\chi_{0.1\%}$, $\chi_{1\%}$, $\chi_{25\%}$, $\chi_{50\%}$, $\chi_{75\%}$, $\chi_{99\%}$, $\chi_{99.9\%}$, for the TMd sampling distribution and sample sizes $n = 5, 10$.

F	n	τ	γ	γ_B	$\chi_{0.1\%}$	$\chi_{1\%}$	$\chi_{25\%}$	$\chi_{50\%}$	$\chi_{75\%}$	$\chi_{99\%}$	$\chi_{99.9\%}$
N(0,1)	5	1.01	0.01	0.00	-1.445	-1.080	-0.312	0.000	0.310	1.088	1.457
	10	1.00	0.00	0.00	-1.044	-0.797	-0.231	0.000	0.229	0.791	1.055
Log(0,1)	5	1.05	-0.01	-0.01	-2.613	-1.929	-0.528	0.001	0.525	1.890	2.638
	10	1.02	0.01	0.02	-1.810	-1.330	-0.374	-0.003	0.379	1.329	1.850
t_3	5	1.18	-0.04	0.00	-1.405	-0.892	-0.221	-0.002	0.219	0.900	1.466
	10	1.05	0.00	0.00	-0.781	-0.556	-0.154	0.000	0.154	0.560	0.790
t_5	5	1.08	0.00	0.00	-1.378	-1.014	-0.276	0.000	0.270	1.014	1.415
	10	1.04	-0.01	0.00	-0.960	-0.692	-0.192	0.000	0.192	0.689	0.956
t_{10}	5	1.05	-0.02	-0.01	-1.454	-1.067	-0.288	0.007	0.297	1.052	1.432
	10	1.01	0.02	0.00	-1.006	-0.738	-0.214	0.001	0.213	0.756	1.007
CN(1%)	5	1.01	0.01	-0.01	-1.489	-1.100	-0.321	0.000	0.313	1.105	1.498
	10	1.01	-0.02	-0.01	-1.052	-0.805	-0.228	0.004	0.232	0.792	1.052
CN(5%)	5	1.03	-0.01	0.01	-1.686	-1.183	-0.328	0.000	0.335	1.179	1.633
	10	0.99	0.00	0.01	-1.050	-0.790	-0.229	0.000	0.231	0.784	1.052
CN(10%)	5	1.07	-0.02	0.00	-1.879	-1.297	-0.357	-0.001	0.341	1.276	1.887
	10	1.00	-0.01	0.01	-1.052	-0.793	-0.229	0.000	0.232	0.795	1.030

From Tables 5-6 we note that the sampling distributions of the R and of the TR statistics are highly positive skewed, even in the normal case. For contaminated normal models with a high percentage of contamination, $CN(5\%)$ and $CN(10\%)$, and for the Student-t models, t_3 and t_5, the sampling distributions of R and TR are heavy tailed, with high positive skewness, and present some asymmetry even in the central part of the distribution, as it is indicated by the obtained value of quartile skewness coefficient, γ_B. However, the distribution of the TR statistic is less asymmetric than the distribution of the R statistic, with a not so long right tail. In all the cases the skewness as well as the tail-weight decrease with the increase

of the sample size n, and we thus advise the use of the TR statistic for large sample sizes. These conclusions are easily observed from the histograms presented in Figures 3-6.

Table 5: Estimates of τ, γ, γ_B, $\chi_{0.1\%}$, $\chi_{1\%}$, $\chi_{25\%}$, $\chi_{50\%}$, $\chi_{75\%}$, $\chi_{99\%}$, $\chi_{99.9\%}$, for the R sampling distribution and sample sizes $n = 5, 10$.

F	n	τ	γ	γ_B	$\chi_{0.1\%}$	$\chi_{1\%}$	$\chi_{25\%}$	$\chi_{50\%}$	$\chi_{75\%}$	$\chi_{99\%}$	$\chi_{99.9\%}$
N(0,1)	5	0.97	0.48	0.06	0.351	0.663	1.699	2.252	2.875	4.628	5.542
	10	1.00	0.39	0.04	1.057	1.459	2.513	3.028	3.582	5.151	5.985
Log(0,1)	5	1.02	0.87	0.10	0.584	1.113	2.880	3.912	5.173	9.365	12.058
	10	1.03	0.81	0.09	1.782	2.452	4.365	5.414	6.679	10.825	13.399
t_3	5	1.39	7.55	0.17	0.248	0.453	1.223	1.738	2.463	6.901	14.763
	10	1.42	5.65	0.19	0.737	0.999	1.926	2.532	3.417	8.971	16.812
t_5	5	1.15	2.03	0.13	0.323	0.560	1.494	2.049	2.773	5.842	8.579
	10	1.16	1.81	0.12	0.915	1.250	2.284	2.887	3.662	6.981	10.203
t_{10}	5	1.04	0.85	0.08	0.350	0.617	1.614	2.183	2.851	5.124	6.592
	10	1.07	0.86	0.08	1.011	1.382	2.434	2.995	3.657	5.957	7.632
CN(1%)	5	1.08	1.19	0.06	0.351	0.664	1.719	2.289	2.927	5.204	8.039
	10	0.98	0.38	0.04	1.080	1.473	2.514	3.028	3.591	5.133	5.922
CN(5%)	5	1.38	1.82	0.10	0.387	0.707	1.793	2.413	3.164	7.477	10.383
	10	0.99	0.39	0.05	1.059	1.470	2.515	3.026	3.589	5.156	5.974
CN(10%)	5	1.30	1.68	0.16	0.400	0.723	1.901	2.585	3.536	8.516	11.470
	10	0.99	0.38	0.05	1.075	1.464	2.515	3.027	3.589	5.144	5.973

Table 6: Estimates of τ, γ, γ_B, $\chi_{0.1\%}$, $\chi_{1\%}$, $\chi_{25\%}$, $\chi_{50\%}$, $\chi_{75\%}$, $\chi_{99\%}$, $\chi_{99.9\%}$, for the TR sampling distribution and sample sizes $n = 5, 10$.

F	n	τ	γ	γ_B	$\chi_{0.1\%}$	$\chi_{1\%}$	$\chi_{25\%}$	$\chi_{50\%}$	$\chi_{75\%}$	$\chi_{99\%}$	$\chi_{99.9\%}$
N(0,1)	5	0.95	0.43	0.05	0.273	0.519	1.321	1.749	2.223	3.507	4.143
	10	0.99	0.28	0.02	0.924	1.277	2.164	2.583	3.023	4.219	4.830
Log(0,1)	5	1.01	0.77	0.09	0.456	0.871	2.242	3.021	3.964	6.956	8.869
	10	1.02	0.66	0.08	1.584	2.128	3.732	4.560	5.531	8.539	10.326
t_3	5	1.34	6.75	0.16	0.193	0.352	0.947	1.336	1.869	4.918	10.139
	10	1.37	4.81	0.16	0.639	0.861	1.628	2.097	2.747	6.540	11.535
t_5	5	1.12	1.75	0.11	0.256	0.439	1.158	1.586	2.122	4.284	6.204
	10	1.12	1.44	0.10	0.816	1.086	1.944	2.422	3.006	5.317	7.523
t_{10}	5	1.02	0.74	0.07	0.266	0.484	1.259	1.693	2.196	3.816	4.841
	10	1.04	0.66	0.06	0.889	1.197	2.080	2.533	3.044	4.684	5.848
CN(1%)	5	1.05	1.00	0.06	0.282	0.524	1.339	1.775	2.264	3.910	5.808
	10	0.98	0.27	0.02	0.946	1.283	1.163	2.585	3.025	4.199	4.753
CN(5%)	5	1.31	1.59	0.10	0.307	0.551	1.401	1.871	2.440	5.420	7.326
	10	0.98	0.27	0.03	0.939	1.276	2.167	2.584	3.029	4.209	4.801
CN(10%)	5	1.25	1.52	0.15	0.318	0.562	1.477	2.000	2.711	6.157	8.100
	10	0.98	0.27	0.03	0.937	1.280	2.163	2.583	3.029	4.198	4.859

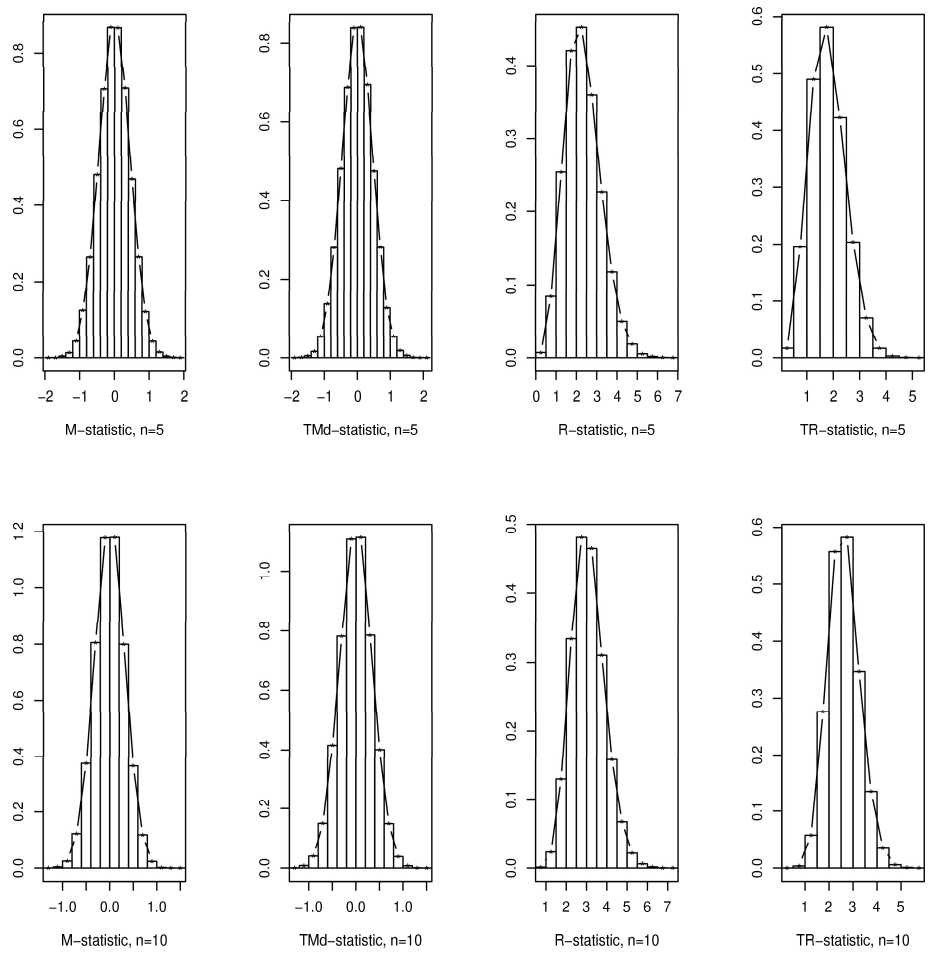

Figure 3: Simulated sampling distribution of the statistics M, TMd, R and TR, for standard normal data and sample sizes 5 and 10.

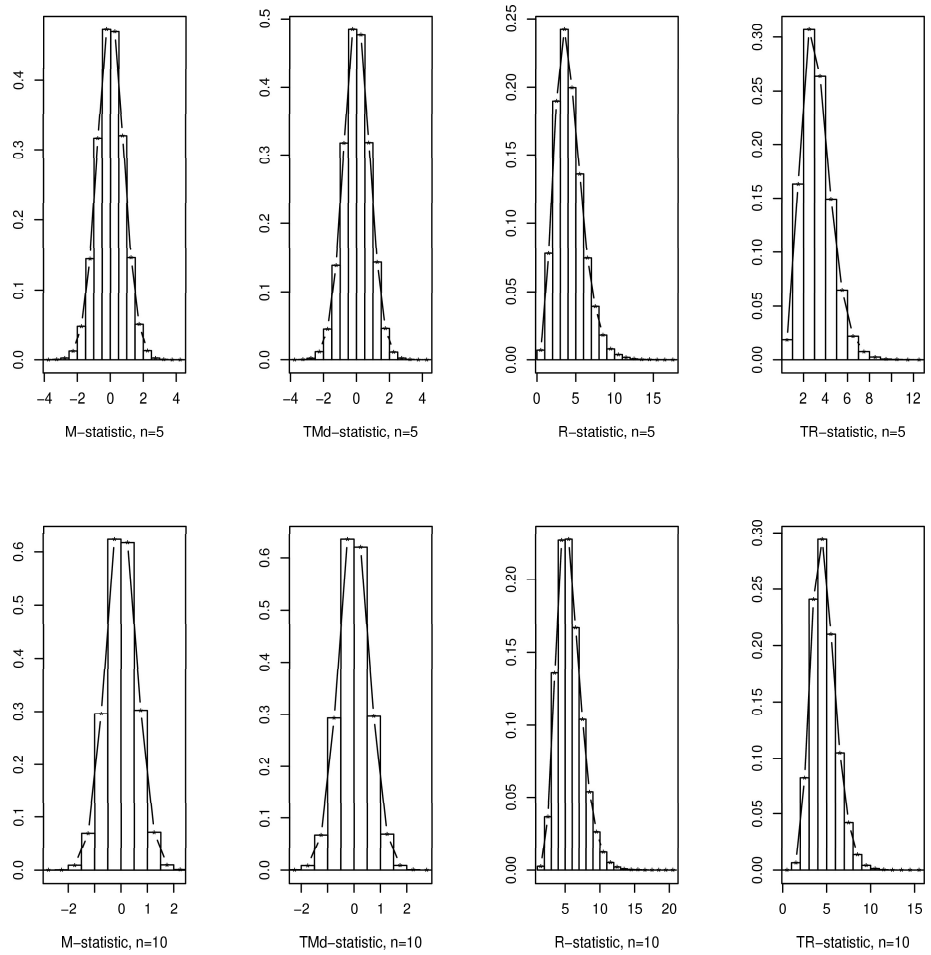

Figure 4: Simulated sampling distribution of the statistics M, TMd, R and TR, for standard logistic data and sample sizes 5 and 10.

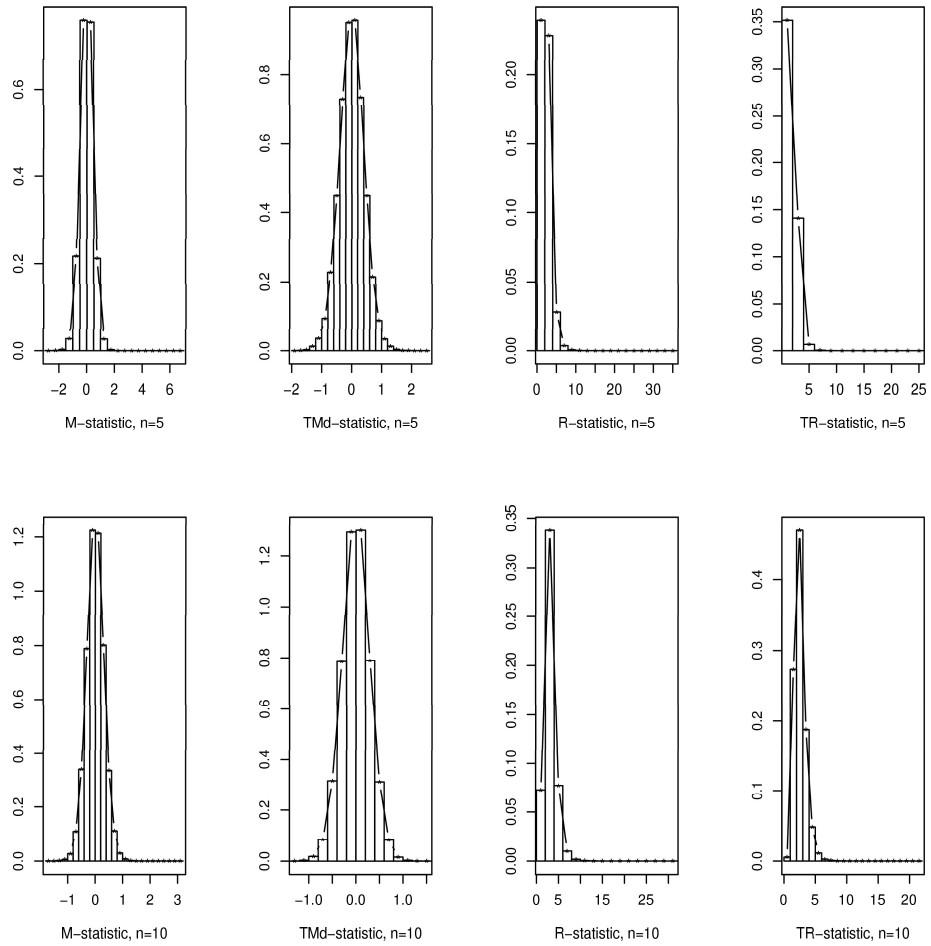

Figure 5: Simulated sampling distribution of the statistics M, TMd, R and TR, for standardized t-student data, t_5, and sample sizes 5 and 10.

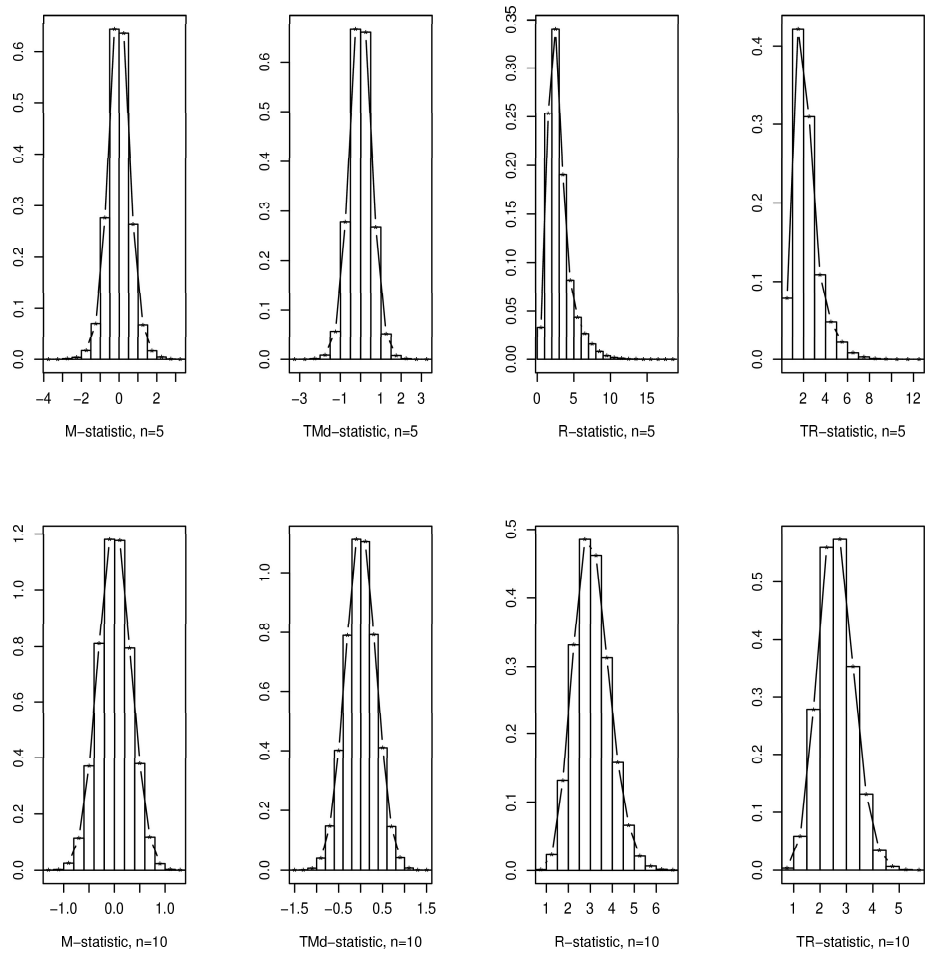

Figure 6: Simulated sampling distribution of the statistics M, TMd, R and TR, for standardized contaminated normal data, $CN(10\%)$, and sample sizes 5 and 10.

The histograms in Figures 3-6 confirm the symmetry of the sampling distributions of M and TMd, and the visible asymmetry of the distributions of R and TR, principally for small samples. The increase of the sample size leads us, in some cases, to a quasi-symmetric distribution (see Figures 3 and 6); for the logistic and the CN(10%) data, the distribution of TR is less asymmetric than the distribution of R; for t_5 data the distribution of the TR presents high asymmetry, even for large sample sizes, although smaller than the asymmetry of the distribution of R.

3 Control charts and simulation results

Whenever implementing a control chart, a practical advice is that a control chart with 3-σ control limits must be avoided if the distribution of the control statistic is very asymmetric; in this case it is preferable to fix the control limits of the chart at probability quantiles of the control statistic distribution. However, the analytical determination of these quantiles is in general impossible to obtain, as well as its estimation, because we do not have sufficient observations for doing it accurately.

The results presented in Subsection 2.2 justify the use, in this study, of two--sided control charts with 3-sigma control limits to monitor the process mean value at a target μ_0. Thus, to detect increases or decreases in the process mean value μ, we implement the M-chart with control limits given in (1.2), and the TMd chart with lower and upper control limits given by

$$LCL_{TMd} = E(TMd) - 3\sqrt{V(TMd)}, \quad UCL_{TMd} = E(TMd) + 3\sqrt{V(TMd)}. \tag{3.1}$$

For standard normal data the limits of the TMd-chart are given by

$$LCL_{TMd} = -3d_{3,TMd}, \quad UCL_{TMd} = 3d_{3,TMd}, \tag{3.2}$$

where $d_{3,TMd}$ is the tabulated constant presented in Table 2.

To monitor the process standard deviation at a target σ_0, and noting that the main interest is to detect increases in σ and not decreases in σ, we implement in this study one-sided control charts, more specifically, the R-chart with upper control limit given in (1.3), and the TR chart with upper control limit given by

$$UCL_{TR} = E(TR) + 3\sqrt{V(TR)}. \tag{3.3}$$

For standard normal data the upper control limit of the R-chart is given by

$$UCL_{TMd} = d_{2,TR} + 3d_{3,TR}, \tag{3.4}$$

where $d_{2,TR}$ and $d_{3,TR}$ are the tabulated constants presented in Table 2.

3.1 Robustness versus performance

The ability of a generic W control chart to detect process changes is usually measured by the expected number of samples taken before the chart signals, i.e., by its

ARL (*Average Run Length*), or alternatively in some cases by its power function, together with the standard deviation of the Run Length distribution, $SDRL$.

Definition 3.1. *When the successive values of the control statistic W are independent, and when we do not have to estimate the control limits of the chart, the RL variable (i.e., the number of samples taken before the chart signals) has a geometric distribution, and the ARL is given by*

$$ARL_{W}(\theta) = \frac{1}{1 - P(W \in C \mid \theta)} =: \frac{1}{\pi_{W}(\theta)}, \tag{3.5}$$

where θ denotes the parameter to be controlled at $\theta = \theta_0$, with $\pi_{W}(\theta)$ the power function of the W-chart. The $SDRL$ is given by

$$SDRL_{W}(\theta) = \frac{\sqrt{P(W \in C \mid \theta))}}{1 - P(W \in C \mid \theta)}. \tag{3.6}$$

Remark 3.1. *Assuming that the process changes from the in-control state, $\theta = \theta_0$, to an out-of-control state, θ, a value in the space parameter, the power function of the chart is the probability of detection of that change in any arbitrary sample.*

Definition 3.2. *When the process is in-control, the power function gives us the false alarm rate of the chart, also called the α-risk, given by*

$$\alpha = P\left(W \notin C \mid IN\right) = P\left(W \notin C \mid \theta = \theta_0\right). \tag{3.7}$$

Remark 3.2. *The control limits of a W-chart are usually determined in order to have a chart with a small fixed false alarm rate (a large in-control ARL) and we hope to obtain high power function values (small out-of-control ARL) for the shifts the chart must detect.*

Remark 3.3. *When we have to estimate some process parameters to determine the control limits of the chart, or if the successive values of the control statistic W are not independent, the RL variable has not anymore a geometric distribution, but a more right-skewed distribution, and the false alarm rate of the chart is not anymore equal to the reciprocal of the in-control ARL. Some authors, see Chakraborti (2006, 2007) for instance, refer that in this case the ARL and the SDRL parameters are not the best measures of performance of a control chart, due the high asymmetry of the RL distribution, and one might prefer the use of the Median Run Length,*

MRL, as a measure performance, and the 5th and the 95th percentiles of the RL distribution to represent the spread of the RL. Additionally, for a more complete understanding of the chart performance, Chakraborti (2000, 2006, 2007) and Jensen et al. (2006), for instance, state that we must analyze the conditional RL distribution, i.e., the RL distribution conditional on the observed estimates, together with the analysis of the marginal RL distribution. Such a marginal distribution is computed by integrating the conditional RL distribution over the range of the parameter estimators and takes thus into account the random variability introduced into the charting procedure through parameter estimation without requiring the knowledge of the observed estimates. Further details about measures of performance of control charts can be found, for instance, in Chakraborti (2000, 2006, 2007) and in Jensen et al. (2006).

In the following study, to analyze the robustness of the previous control charts to the normality assumption, implemented with exact control limits,

1. we consider, to describe the data process, standardized data of the symmetric distributions in set D (see Subsection 2.2);

2. we implement the charts with the control limits given in (1.2), (1.3), (3.2) and (3.4), for sample sizes $n = 5, 10$;

3. we compute the false alarm rates, α, defined in (3.7), by Monte Carlo simulation techniques, using a sample of 500,000 values of the control statistic for each of the 30 replicates of the simulation experiment; this procedure allows us to present the α values with a precision of 4 decimal figures; finally, we compare them with the expected value α_0, obtained for normal data.

The obtained simulated false alarm rates are presented in Tables 7-8 for sample sizes $n = 5, 10$; in each line we underline the α-value associated to the most robust chart. While the $\overline{X}$-chart is non-robust to the normality assumption, the TMd chart for $n = 5$ is quasi-robust, except for contaminated normal distributions; the TR-chart cannot be considered robust, but even so, it is more robust than the R-chart. The worst results are obtained when we consider contaminated normal data. Indeed, when there is a chance of having this distributional situation it is better to implement the TMd and the TR charts for sample sizes $n = 10$.

Table 7: False Alarm rates of the $\overline{X}$ and TMd charts.

Model F	τ	$\overline{X}_{n=5}$	$TMd_{n=5}$	$\overline{X}_{n=10}$	$TMd_{n=10}$
N(0,1)	1.00	.00270	.00272	.00269	.00272
t_{10}	1.15	.00392	.00265	.00333	.00179
Log(0,1)	1.21	.00430	.00263	.00364	.00154
t_5	1.34	.00655	.00245	.00508	.00095
t_3	1.72	.01063	.00187	.00912	.00019
CN(1%)	1.03	.00540	.00336	.00478	.00302
CN(5%)	1.20	.01198	.00591	.01018	.00429
CN(10%)	1.54	.01543	.00845	.01347	.00589

Table 8: False Alarm rates of the R and TR charts.

Model F	τ	$R_{n=5}$	$TR_{n=5}$	$R_{n=10}$	$TR_{n=10}$
N(0,1)	1.00	.00452	.00402	.00423	.00315
t_{10}	1.15	.01327	.01090	.01965	.01392
Log(0,1)	1.21	.01523	.01232	.02320	.01620
t_5	1.34	.02439	.02010	.04134	.03007
t_3	1.72	.03197	.02651	.05725	.04191
CN(1%)	1.03	.01397	.01249	.02175	.01784
CN(5%)	1.20	.03904	.03498	.06734	.05661
CN(10%)	1.54	.05352	.04811	.09268	.07934

The analysis of the performance of the previous charts to detect changes in the process parameters is evaluated in terms of the obtained power function values of the chart, defined in (3.5) for some different magnitude changes.

The obtained simulated power function values are presented in Tables 9-10 for sample size $n = 10$; for every magnitude of change and each model, we underline the highest obtained value, which corresponds to the most powerful chart. These results lead us to the following conclusions: the TMd (and the TR) chart is more

robust than the $\overline{X}$ (and the R) chart, with smaller false alarm rates; when the tails of the underlying model become heavier, the TMd (and the TR) chart is able to overpass the $\overline{X}$ (and the R) chart in terms of performance to detect large changes. The conclusions are similar for $n = 5$, although we obtain larger power function values when we consider $n = 10$, i.e., the charts implemented for sample sizes $n = 10$ are able to detect the occurred changes more quickly.

Table 9: Power function values of the charts ($n = 10$, $\mu \to \mu_1$, $\sigma = 1$).

μ_1	$\overline{X}$	TMd	$\overline{X}$	TMd	$\overline{X}$	TMd	$\overline{X}$	TMd
	N(μ_1,1)		t_3		t_5		t_{10}	
0.5	.0780	.0629	.0625	.0148	.0749	.0372	.0771	.0513
1	.5646	.4750	.5758	.4622	.5672	.4700	.5652	.4731
2	.9996	.9980	.9971	.9999	.9988	.9993	.9994	.9987
2.5	1.000	1.000	.9993	1.000	.9999	1.000	1.000	1.000
3	1.000	1.000	.9998	1.000	1.000	1.000	1.000	1.000
	Log(μ_1,1)		CN(1%)		CN(5%)		CN(10%)	
0.5	.0771	.0471	.0841	.0642	.1010	.0702	.1122	.0767
1	.5654	.4725	.5630	.4753	.5591	.4755	.5561	.4767
2	.9993	.9988	.9990	.9978	.9975	.9969	.9966	.9959
2.5	.9999	1.000	.9999	.9999	.9999	.9999	.9999	1.000
3	1.000	1.000	1.000	1.000	1.000	1.000	1.000	1.000

Table 10: Power function values of the charts ($n = 10$, $\mu = 0$, $\sigma \to \sigma_1$).

σ_1	R	TR	R	TR	R	TR	R	TR
	N(0,σ_1)		t_3		t_5		t_{10}	
1.25	.0616	.0647	.1199	.0984	.1227	.1081	.0971	.0910
1.5	.2277	.2557	.2087	.1869	.2542	.2491	.2510	.2614
2	.6458	.6965	.4307	.4258	.5646	.5883	.6162	.6549
2.5	.8730	.9023	.6409	.6546	.7903	.8181	.8426	.8720
3	.9564	.9688	.7924	.8119	.9071	.9255	.9395	.9546
	Log(0,σ_1)		CN(1%)		CN(5%)		CN(10%)	
1.25	.1075	.0987	.0904	.0925	.1734	.1739	.2320	.2334
1.5	.2621	.2673	.2589	.2861	.3519	.3778	.4235	.4497
2	.6122	.6447	.6636	.7120	.7185	.7603	.7629	.7998
2.5	.8330	.8608	.8799	.9076	.9016	.9246	.9194	.9387
3	.9327	.9482	.9588	.9706	.9666	.9763	.9731	.9810

4 Monitoring a cork process production

For monitoring on-line a cork stopper's process production, more precisely, the cork stoppers caliber 45 mm $\times$ 24 mm, we have implemented control charts with estimated control limits for sample size $n = 10$, in order to monitor the process mean value and the process standard deviation. The corks must have a target mean length $\mu_{0,L} = 45$ mm, with a tolerance interval of 45 ± 1 (mm), and a target mean diameter $\mu_{0,D} = 24$ mm, with a tolerance interval of 24 ± 0.5 (mm).

To estimate the control limits of the charts used to monitor this process production, here denoted by M, M^*, TMd, R, R^* and TR charts, we carry out the following procedure:

1. we consider $m = 25$ and $m = 50$ initial subgroups of size $n = 10$, taken when the process is considered stable and IN-control;

2. from these initial subgroups we compute m partial estimates ($j = 1, \cdots, m$) of the interest parameters, here denoted μ_0 and σ_0, through the use of the

TMd and TR estimators as well as the use of the usual estimators, the sample mean $\overline{X}$ and the sample range R; to obtain unbiased partial estimates, $\widehat{\sigma}_{0j}$, whenever the underlying model is normal, we divide the statistics R and TR by its mean values, d_2 and $d_{2,TR}$, respectively, whenever the underlying model is normal, given in Table 2; we also compute estimates of $E(TMd)$, $E(TR)$, $V(TMd)$ and $V(TR)$;

3. then, we compute overall estimates to be used in the control limits, presented in Table 11, by averaging the estimates obtained in step 2.

Table 11: Implemented control charts for monitoring the cork's process production, for sample sizes $n = 10$, and $m = 25, 50$.

Chart	Control limits	Parameters' estimates
M	$\widehat{\mu}_0 \pm 3\frac{\widehat{\sigma}_0}{\sqrt{n}}$	$\widehat{\mu}_0 = \frac{1}{m}\sum_{j=1}^{m} \overline{X}_j$ $\widehat{\sigma}_0 = \frac{1}{m}\sum_{j=1}^{m} R_j/d_2$
M^*	$\widehat{\mu}_0^* \pm 3\frac{\widehat{\sigma}_0^*}{\sqrt{n}}$	$\widehat{\mu}_0^* = \frac{1}{m}\sum_{j=1}^{m} TMd_j = \overline{TMd}$ $\widehat{\sigma}_0^* = \frac{1}{m}\sum_{j=1}^{m} TR_j/d_{2,TR}$
TMd	$\widehat{E(TMd)} \pm 3\sqrt{\widehat{V(TMd)}}$	$\widehat{E(TMd)} = \frac{1}{m}\sum_{j=1}^{m} TMd_j$ $\widehat{V(TMd)} = \frac{1}{m-1}\sum_{j=1}^{m}\left(TMd_j - \overline{TMd}\right)^2$
R	$\overline{R} + 3d_3\widehat{\sigma}_0$	$\widehat{\sigma}_0 = \frac{1}{m}\sum_{j=1}^{m} R_j/d_2$
R^*	$\overline{R} + 3d_3\widehat{\sigma}_0^*$	$\widehat{\sigma}_0^* = \frac{1}{m}\sum_{j=1}^{m} TR_j/d_{2,TR}$
TR	$\widehat{E(TR)} + 3\sqrt{\widehat{V(TR)}}$	$\widehat{E(TR)} = \frac{1}{m}\sum_{j=1}^{m} TR_j = \overline{TR}$ $\widehat{V(TR)} = \frac{1}{m-1}\sum_{j=1}^{m}\left(TR_j - \overline{TR}\right)^2$

We note that the M and the M^* charts have the same control statistic, $\overline{X}$, but we have considered different estimates for the targets, the usual ones or robust estimates to determine the control limits; the same happens with the R and the R^* charts that have the same control statistic, R, but different upper control limit. The statistic $\overline{R}$ that appears in the control limit of the R and of the R^* charts corresponds to the average of the sample ranges of the m initial subgroups, and the constant d_3 denotes the standard deviation of R whenever the underlying model is normal. As already mentioned, its value is given in Table 2.

For the study we have considered a sample of the cork's length and the cork's diameter values, of size 1250; the first 750 values of the sample were used to estimate the control limits of the charts, and the remaining 500 values were used to implement the charts and to analyze its robustness. Here we only present the results of the analysis of the cork's length dataset, which are similar to the ones obtained for the cork's diameter.

After a brief exploratory data analysis of the cork's length dataset we conclude that all the length's data are within the tolerance interval fixed by the production director. The shape of the histograms associated to the data of the initial subgroups (datasets of size $m \times n = 25 \times 10 = 250$ and $m \times n = 50 \times 10 = 500$) used to estimate the control limits of the charts suggest we are working with non-normal data, and the same conclusion is suggested by the Q-Q normal plots, that present several points outside the straight line. In order to confirm or to deny the previous conclusion, we apply a Shapiro-Wilk normality test to these subgroup datasets, and we estimate the tail-weight and the asymmetry of the underlying distribution. Thus, we do not reject the normality of the data of the $m = 25$ initial subgroups (for which we got a p-value=0.165 and a small value for the estimate of the Fisher skewness coefficient in (2.6), $\gamma = 0.097$), but we reject the normality of the data of the $m = 50$ initial subgroups (for which we got a p-value=0.003 and a large value for the estimate of the skewness coefficient, $\gamma = 0.317$). For both datasets we got an estimated tail-weight, given in (2.5), less than 1 and equal to $\tau = 0.636$ and $\tau = 0.538$, respectively; therefore we conclude that the normal distribution present heavier tails than the tails of the underlying process distribution.

In Figures 7-8 we present the charts implemented to monitor the cork's length. We remember that all of the observations used to calculate the points represented in these charts are within the tolerance intervals, and thus any point that falls outside the control limits of the charts is associated to a false alarm. From these figures we observe that there is no significant difference between the M and the M^* charts, and well as between the R and the R^* charts; thus, for these initial subgroups datasets there is no benefit of using a robust estimate for the targets instead of the usual ones. Note that these subgroups of data are very homogeneous, with all of the observations between the too-tight tolerance interval, and the standard deviation of the cork's length in each subgroup is very small.

The M and the TMd charts as well as the R and the TR charts represented in Figure 7 do not differ significantly, although we note that the control limits of these charts were estimated through the use of a small number of initial subgroups ($m = 25$) with approximately normal data. Relatively to the charts represented in Figure 8 we observe that the TMd and the TR charts are more robust than the $\overline{X}$ and the R charts. The $\overline{X}$ charts present several points associated to false alarms, which does not happen with the TMd chart, and the points represented in the usual control charts are closer to the control limits than in the robust control charts. In this case the control limits of these charts were estimated through the use of a larger number of initial subgroups ($m = 50$) with non-normal skewed data, a different framework from the one associated to the implementation of the charts in Figure 7.

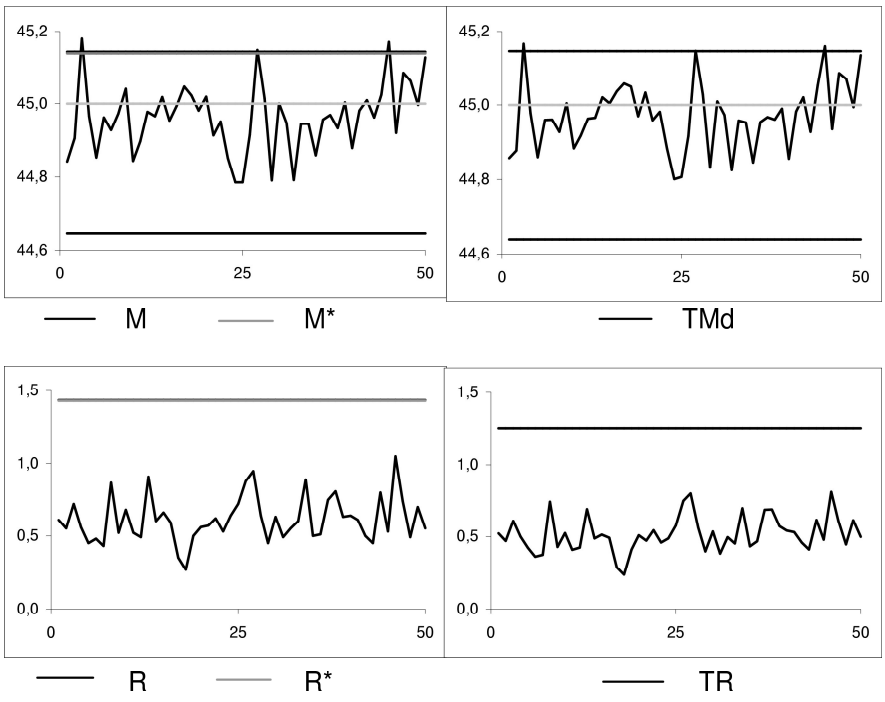

Figure 7: Charts to monitor the cork stopper's length, $n = 10$ and $m = 25$.

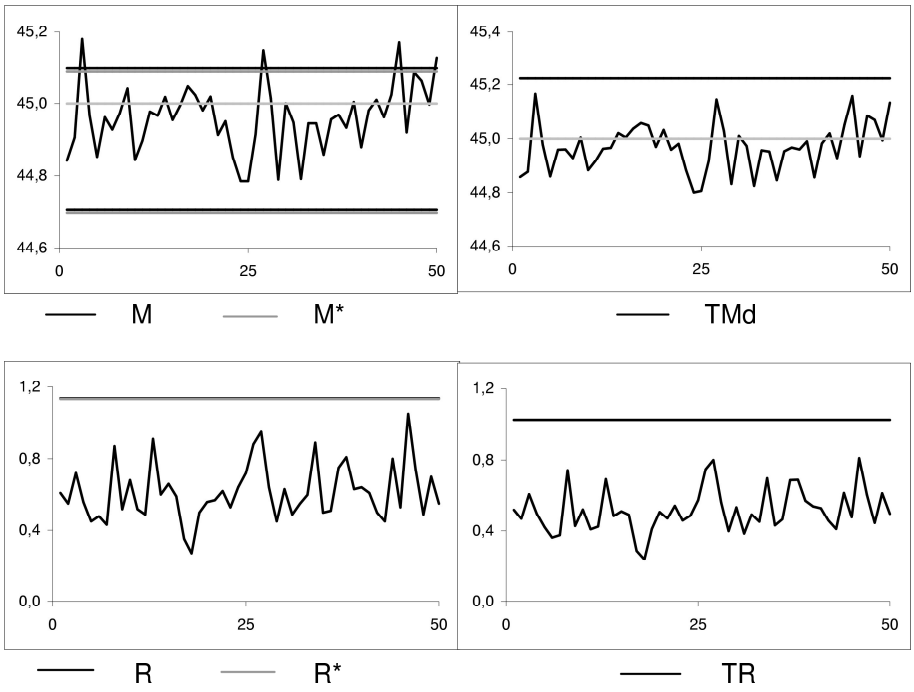

Figure 8: Charts to monitor the cork stopper's length, $n = 10$ and $m = 50$.

From this study we can draw the following overall conclusions: the usual $\overline{X}$ and R charts to monitor non-normal data present simulated alarm rates very different from the expected values, i.e., the non-normality of the underlying data process can have a significant effect on the performance of the charts, and therefore their use deserves careful attention. The use of robust control charts based on the total median and on the total range statistics, for instance, instead of the traditional sample mean and sample range control charts, implemented for moderate samples (say, $n = 10$), can be an adequate alternative to monitor non-normal data. When we have to estimate the control limits of the charts we advise the use of a large number of initial subgroups for the estimation (say $m = 50$, at least) together with the use of robust estimators, in order to obtain adequate estimates even when we have some outliers or contaminated data in the initial subgroups.

Acknowledgments

This work was partially supported by FCT.

References

[1] Amin, R. W. and Lee, S. J. (1999). The Effects of Autocorrelation and Outliers on Two-Sided Tolerance Limits. *J. Quality Technology* **31**(3), pp. 286-300.

[2] Balakrishnan, N. and Kocherlakota, S. (1986). Effects of nonnormality on $\overline{X}$ charts: single assignable cause model. it Dankhya: The Indian Journal of Statistics **48**(B), pp. 439-444.

[3] Chan, L. K., Hapuarachchi, K. P. and Macpherson, B. D. (1988). Robustness of $\overline{X}$ and R charts. *IEEE Transactions on Reliability* **37**(1), pp. 117-123.

[4] Champ, W. C. and Jones, A. L. (2004). Design Phase I $\overline{X}$ charts with Small Sample Sizes. *Quality and Reliability Mathematical Engineering International*, **20**, pp. 497-510.

[5] Chakraborti, S. (2000). Run length, average run length and false alarm rate of Shewhart $\overline{X}$ chart: exact derivations by conditioning. *Communications in Statistics – Simulation and Computation*, **29**1, pp. 61-81.

[6] Chakraborti, S. (2006). Parameter Estimation and Design Considerations in Prospective Applications of the $\overline{X}$ Chart. *Journal of Applied Statistics*, **33**4, pp. 439-459.

[7] Chakraborti, S. (2007). Run Length Distribution and Percentiles: The Shewhart Chart With Unknown Parameters. *Quality Engineering*, **19**, pp. 119-127.

[8] Cox, M. G. and Iguzquiza, E. P. (2001). The total median and its uncertainity. In Ciarlini et al. (eds.), *Advanced Mathematical and Computational Tools in Metrology*, **5**, pp. 106-117.

[9] Figueiredo, F. (2003a). *Controlo Estatistico da Qualidade e Metodos Robustos.* Ph.D. Thesis. Faculty of Science, Lisbon university.

[10] Figueiredo, F. (2003b). Robust estimators for the standard deviation based on a bootstrap sample. *Proc. 13th European Young Statisticians Meeting*, pp. 53-62.

[11] Figueiredo, F. and Gomes, M. I. (2004). The total median is Statistical Quality Control. *Applied Stochastic Models in Business and Industry* **20**, pp. 339-353.

[12] Figueiredo, F. and Gomes, M. I. (2006). Box-Cox Transformations and Robust Control Charts in SPC. In Pavese et al. (eds.), *Advanced Mathematical and Computational Tools in Metrology*, **7**, pp. 35-46.

[13] Hoaglin, D. M., Mosteller, F. and Tukey, J. W. (1983). *Understanding Robust and Exploratory Data Analysis.* Wiley, New York.

[14] Hampel, F. R. (1971). A general qualitative definition of robustness. *Annals of Mathematical Statistics*, **42**, pp. 1887-1896.

[15] Hampel, F. R., Ronchetti, E. M., Rousseew, P.J. and Stahel, W. (1986). *Robust Statistics: The Approach Based on Influence Functions.* Wiley, New York.

[16] Jensen, W. A., Jones-Farmer, L. A., Champ, C. H. and Woodall, W. H. (2006). *Effects of Parameter Estimation on Control Chart Properties: A Literature Review. J. Quality Technology* **38**, pp. 349-364.

[17] Lax, D. A. (1985). Robust estimators of scale: finite sample performance in long-tailed symmetric distributions. *J. Amer. Statist. Assoc.* **80**, pp. 736-741.

[18] Montgomery, D. C. (2005). *Introduction to Statistical Quality Control.* Wiley, New York.

[19] Nedumaran, G. and Pignatiello, J. J. (2001). *On Estimating $\overline{X}$ Control Limits. J. Quality Technology* **33**(2), pp. 206-212.

[20] Quesenberry, D. C. (1993). *The Effect of Sample Size on Estimated Limits for $\overline{X}$ and X Control Charts. J. Quality Technology* **25**(4), pp. 237-247.

[21] Rocke, D. M. (1989). Robust control charts. *Technometrics* **31**(2), pp. 173-184.

[22] Rocke, D. M. (1992). $\overline{X}_Q$ and R_Q charts: robust control charts. *The Statistician* **41**, pp. 97-104.

[23] Ryan, T. P. (2000). *Statistical Methods for Quality Improvement.* Wiley, New York.

[24] Schilling, E. G. and Nelson, P. R. (1976). *The Effect of Non-Normality on the Control Limits of the $\overline{X}$ Charts. J. Quality Technology* **8**(4), pp. 183-188.